Articles

Role of t_{2g} versus e_g Interactions in the Physical Properties of A_2OBO_3 (A = Mn, Fe)

B. Rivas-Murias,[†] F. Rivadulla,[‡] M. Sánchez-Andújar,*[,§] A. Castro-Couceiro,[§] M. A. Señarís-Rodríguez,[§] and J. Rivas[†]

Departamento Física Aplicada and Departamento Química-Física, Universidade de Santiago de Compostela, 15782 Santiago de Compostela, Spain, and Departamento Química Fundamental, Universidade de A Coruña, 15071 A Coruña, Spain

Received April 26, 2006. Revised Manuscript Received July 10, 2006

From electron spin resonance (ESR), magnetization, and thermoelectric power on the isostructural Mn_2OBO_3 and Fe_2OBO_3, we have been able to establish important differences between the magnetic properties of these two compounds. These differences are rationalized on the basis of t_{2g} versus e_g electronic interactions, orbital occupancy, and structure. For Mn_2OBO_3, we propose the possibility of fast electron transfer between the Mn^{2+} and Mn^{3+} cations, in a similar way to the 3+/4+ Zener pairs in manganites. In the Fe_2OBO_3 system, our main findings are the observation of a magnetization reversal at low field and the observation of the spatially inhomogeneous short-range charge-order state that becomes truly long-range only below the Néel temperature. The phase diagram of both compounds is reconsidered on the basis of these results.

Introduction

Transition metal oxides present an interesting variety of magnetic and transport properties that arise from the strong interplay between spin, orbital, lattice, and charge degrees of freedom. In particular, occupancy and ordering of different transition-metal orbitals (t_{2g} vs e_g) determines the physical properties of the material to a great extent.[1]

Manganese perovskites have been extensively studied during several decades now for this reason.[2] In this case, the active e_g orbitals are strongly coupled to the lattice, and a strong Jahn−Teller distortion normally sets up at much higher temperature than the magnetic ordering ($T_{OO} > T_N$). On the other hand, vanadium perovskites are prototypical t_{2g} systems, in which both Jahn−Teller and crystal field splitting are weaker than in e_g orbitals ($T_N \approx T_{OO}$). Moreover, orbital angular momentum is not necessarily quenched for t_{2g} electrons, which leads to interesting effects related to spin−orbit coupling.

In principle, a similar approach could be followed in warwickite $A^{2+}A^{3+}OBO_3$ (A = Mn, Fe), which represents a series of materials in which charge, magnetic, and orbital ordering can be realized at different orbitals in the same structure. In these compounds, where (both $Mn^{2+/3+}$ and $Fe^{2+/3+}$ are in the high spin state) Fe^{3+} and Mn^{2+} cations present the same electronic configuration ($t_{2g}^3e_g^2$), there is an extra electron in a t_{2g} orbital of the Fe^{2+} cation ($t_{2g}^4e_g^2$) and a hole in the e_g orbital of the Mn^{3+} cation ($t_{2g}^3e_g^1$). This could be the source of important differences in the physical properties of the materials.

The warwickite structure is characterized by the presence of one-dimensional ribbons of edge sharing AO_6 octahedra.[3,4] The ribbons are connected by corner sharing and the trigonal planar BO_3 groups, defining two inequivalent sites for the octahedral metal ions, A(1) and A(2), as can be seen in Figure 1.

In Mn_2OBO_3, a strong Jahn−Teller distortion with an axial elongation of the $Mn(1)O_6$ octahedra[5] suggests a charge ordering of the kind $Mn^{3+}(1)-Mn^{2+}(2)$ and d_z^2 orbital ordering at the Mn(1) site. Specific heat and magnetization studies have shown an antiferromagnetic (AF) transition at $T_N = 105$ K[6] and weak ferromagnetic behavior below 70 K. Nevertheless, on the basis of more recent neutron diffraction results, Goff et al.[7] argue that long-range AF order occurs only below 26 K and that the other transitions reported are due to impurity phases, so that this point remains a controversial issue.

On the other hand, Fe_2OBO_3 has been reported to become charge ordered (electrostatically driven) below 317 K.[8] At

* Corresponding author. Tel.: (+34) 981167000. Fax: (+34) 981167065. E-mail: msanchez@udc.es.
[†] Departamento Física Aplicada, Universidade de Santiago de Compostela.
[‡] Departamento Química-Física, Universidade de Santiago de Compostela.
[§] Universidade de A Coruña.

(1) Tokura, Y.; Nagaosa, N. *Science* **2000**, *288*, 462.
(2) Goodenough, J. B. *Phys. Rev.* **1955**, *100*, 564.
(3) Bertaut, E. F. *Acta Crystallogr.* **1950**, *3*, 473.
(4) Takeuchi, Y.; Watanabe, T.; Ito, T. *Acta Crystallogr.* **1950**, *3*, 98.
(5) Norrestam, R.; Kritikos, M.; Sjödin, A. *J. Solid State Chem.* **1995**, *114*, 311.
(6) Continentino, M. A.; Pedreira, A. M.; Guimarães, R. B.; Mir, M. J.; Fernandes, C. *Phys. Rev. B* **2001**, *64*, 14406.
(7) Goff, R.; Williams, A. J.; Attfield, J. P. *Phys. Rev. B* **2004**, *70*, 14426.

10.1021/cm0609698 CCC: $33.50
Published on Web 08/16/2006

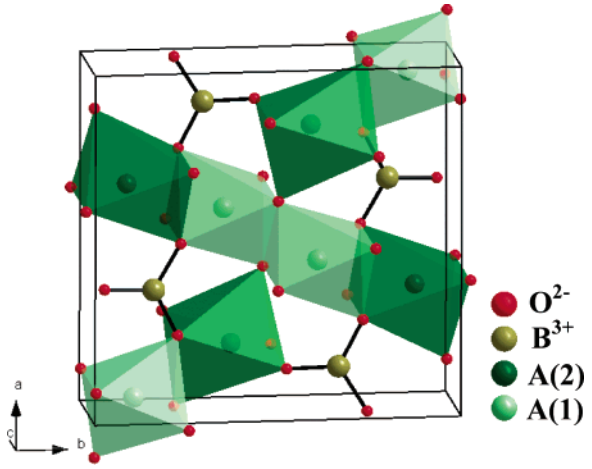

Figure 1. $A^{2+}A^{3+}OBO_3$ warwickite structure. The metals cations are octahedrally coordinated, with the octahedra sharing edges to form ribbons, linked by corner sharing and the trigonal planar BO_3 groups.

this temperature the compound shows a structural distortion from orthorhombic (*Pmcn*) to monoclinic ($P2_1/c$) symmetry; the divalent and trivalent ions are equally distributed over the two crystallographic sites, giving the chemical formula $Fe^{2+}(1)_{0.5}Fe^{3+}(1)_{0.5}Fe^{2+}(2)_{0.5}Fe^{3+}(2)_{0.5}OBO_3$. The structural distortion and a small jump in the resistivity (with a very small increase in the activation energy) are the main findings supporting the existence of charge ordering. However, ^{57}Fe Mössbauer spectra[9−11] show that only below 270 K fast electron transfer between Fe^{2+} and Fe^{3+} is suppressed. Moreover, the mean Fe(1)−O and Fe(2)−O distances are equal, and X-ray and neutron diffraction do not show evidence of long-range charge ordering.[9,12] In agreement with this scenario, Attfield et al.[8] suggested that charge ordering in this material is short-ranged, extending only ≈ 10−100 Å. Below $T_N = 155$ K Fe_2OBO_3 orders antiferromagnetically, with the magnetic moments on the Fe(1) and Fe(2) chains antiparallel so that a small ferromagnetic moment of 0.06 μ_B per formula unit results.[12]

Here we present electron spin resonance (ESR), magnetization, and thermoelectric power data for Fe_2OBO_3 and Mn_2OBO_3. On the basis of our results, a complete revision of the phase diagram of these compounds is presented. The different phases are rationalized on the basis of the role of e_g electrons in the Mn sample versus that of the t_{2g} electrons in the Fe sample.

Experimental Section

Polycrystalline Mn_2OBO_3 was synthesized by heating in air pressed pellets of stoichiometric amounts of $MnCO_3$ and H_3BO_3 at 700 °C for 60 h and at 800 °C for 24 h, with intermediate grindings.[5]

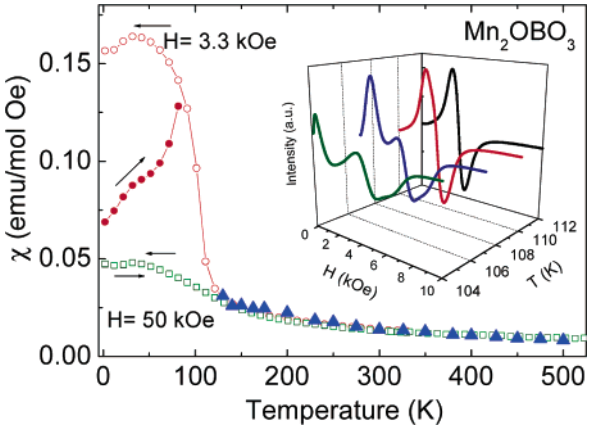

Figure 2. ZFC−FC susceptibility of Mn_2OBO_3 measured at two different fields $H = 3.3$ kOe and $H = 50$ kOe. The closed triangles represent the susceptibility obtained by ESR (as explained in the text). Inset: X-band ESR lines between 112 and 104 K.

Fe_2OBO_3 was synthesized by heating pressed pellets of a stoichiometric mixture of $FeBO_3$, Fe_2O_3, and Fe in a sealed evacuated silica tube at 800 °C for 110 h with intermediate grindings. $FeBO_3$ had been previously obtained by firing Fe_2O_3 and H_3BO_3 in air at 700 °C, following the method reported in ref 12.

In both samples, X-ray powder diffraction (XRPD) confirmed the formation of the warwickite-type structure. This is the only phase present in the case of the Fe material, while in the case of the Mn sample it appears impurified by a small amount (<2%) of Mn_2O_3. The XRPD patterns were analyzed by the Rietveld method, using the Rietica software.[13]

The Fe sample was refined in the space group $P2_1/c$ using the initial model proposed by Attfield et al.,[12] while for the Mn sample we used the space group $P2_1/n$ and the model proposed by Norrestam et al.[5] In both cases the bond lengths obtained are in good agreement with those reported in the literature.[5,9]

The temperature dependence of the molar magnetic susceptibility, χ_m, was measured from 5 to 300 K in different magnetic fields (from 9 Oe to 50 kOe) both on heating from low temperature after cooling in zero magnetic field (ZFC) and after cooling in a field (FC), in a MMS and in a PPMS magnetometer, both of Quantum Design.

In the case of Mn_2OBO_3, additional χ_m measurements were also carried out in a vibrating sample magnetometer (VSM) from 300 to 1000 K ($H = 10$ kOe).

ESR spectra were taken in a Bruker EMX EPR spectrometer at 9.4 GHz (X-Band) between 104 and 500 K.

Results and Discussion

Mn_2OBO_3. In Figure 2, we show the ZFC−FC susceptibility, $\chi(T)$, at two different magnetic fields. In agreement with the literature,[6] we observe an increase of the magnetization below $T \approx 105$ K. Below $T \approx 80$ K the ZFC−FC curves split, and the ZFC curve becomes strongly temperature dependent, suggesting some sort of "glassy" behavior in this material. The FC data show a maximum around 30 K, which corresponds with the long-range atomic force microscopy reported by Goff et al.[7] For high fields (50 kOe), the absolute

(8) Attfield, J. P.; Bell, A. M. T.; Rodríguez-Martínez, L. M.; Greneche, J. M.; Cernik, R. J.; Clarke, J. F.; Perkins, D. A. *Nature* **1998**, *396*, 655.
(9) Attfield, J. P.; Bell, A. M. T.; Rodríguez-Martínez, L. M.; Greneche, J. M.; Retoux, R.; Leblanc, M.; Cernik, R. J., Clarke, J. F.; Perkins, D. A. *J. Mater. Chem.* **1999**, *9*, 205.
(10) Douvalis, A. P.; Papaefthymiou, V.; Moukarika, A.; Bakas, T.; Kallias, G. *J. Phys.: Condens. Matter* **2000**, *12*, 177.
(11) Douvalis, A. P.; Papaefthymiou, V.; Moukarika, A.; Bakas, T. *Hyperfine Interact.* **2000**, *126*, 319.
(12) Attfield, J. P.; Clarke. J. F.; Perkins, D. A. *Physica B* **1992**, *180−181*, 581.
(13) Howard, C. J.; Hunter, B. A. *Rietica: A Computer Program for Rietveld Analysis of X-ray and Neutron Powder Diffraction Patterns*. Australian Nuclear Science and Technology Organization, Lucas Heights Research Laboratories: 1997.

value of the susceptibility decreases, and the ZFC−FC splitting disappears. Also, the ZFC and FC curves show a maximum around 30 K.

The nature of the magnetic phase transition at 105 K and even its intrinsic character is a matter of debate. On one hand, Goff et al.[7] suggested that long-range AF order occurs below 26 K, and other apparent magnetic transitions are due to secondary phases. On the other hand, Continentino et al.[6] reported a peak at 105 K in the specific heat of Mn_2OBO_3, whose magnitude is consistent with a bulk magnetic transition.

Here we provide a strong experimental support for the latter scenario. ESR spectra of Mn_2OBO_3 have been recorded from 500 K, approaching the magnetic transition at 105 K. A single Lorentzian line centered at $g = 1.99$ is observed at high temperature (see Figure 2, inset). Between 110 and 107 K, the ESR line becomes severely distorted. The intensity of the ESR line is proportional to the magnetic susceptibility,[14] so by comparing it with a reference, the absolute value of $\chi_{ESR}(T)$ can be derived from this experiment. We have used a polycrystalline sample of $La_{0.67}Ca_{0.33}MnO_3$ as a reference, in which both Mn^{3+} and Mn^{4+} are known to contribute to the resonance line[15] and whose line width is similar to that of the Mn oxyborate. The intensity was determined approximating the area by the product $\Delta H_{pp}(T)^2 h_{pp}(T)$, where $\Delta H_{pp}(T)$ is the peak-to-peak line width and h_{pp} is the peak-to-peak amplitude of the measured derivative signal.

The results are shown in Figure 2; there is a perfect agreement between $\chi(T)$ above 110 K determined by ESR and that determined by conventional direct current (dc) magnetometry. This indicates that both Mn^{3+} and Mn^{2+} are contributing to the resonance line as a single entity. The strong distortion of the high-temperature line below 110 K indicates then the intrinsic character of the transition, in agreement with the report by Continentino et al.[6] On the basis of these results and the glassy behavior observed in the dc susceptibility, the most probable scenario is an inhomogeneous AF ordering below ≈ 110 K, in which the Mn^{3+}−Mn^{2+} pairs would order antiparallel, as in the magnetic structure obtained by Goff et al.[7]

On the other hand, the time scales associated with the Mn^{3+}−Mn^{2+} fast electron transfer must be of the order of ESR, while XRPD can only see the average distorted structure. This is an important result, as it points toward the possibility of a fast electron transfer between Mn^{2+}−Mn^{3+} pairs, in a manner similar to that of the Mn^{3+}−Mn^{4+} Zener polarons in manganites, in spite of the larger Coulomb repulsion.

From the fitting to a Curie−Weiss law up to 1000 K we derived a value of $\mu_{eff} = 6.6(4)\ \mu_B$. This is much larger than the free-ion value, which supports the hypothesis of pair correlations in the paramagnetic state.

Looking at the crystallographic structure of Mn_2OBO_3, there are two Mn−Mn distances inside the ribbons: a shorter $A^{3+}(1)$−$A^{3+}(1)$ distance and a longer $A^{3+}(1)$−$A^{2+}(2)$ distance. At room temperature these distances are ≈2.86 Å and ≈3.32 Å, respectively, too long for a direct t_{2g}−t_{2g} orbital overlap.[16] On the other hand, indirect Mn^{2+}−O−Mn^{3+} exchange between the Mn^{3+} of one ribbon and the Mn^{2+} of the other ribbon must be possible as Mn^{3+}−O^{2-}−Mn^{2+} ions lie in a plane parallel to the *ab* plane and the angle between these cations is ≈125°.

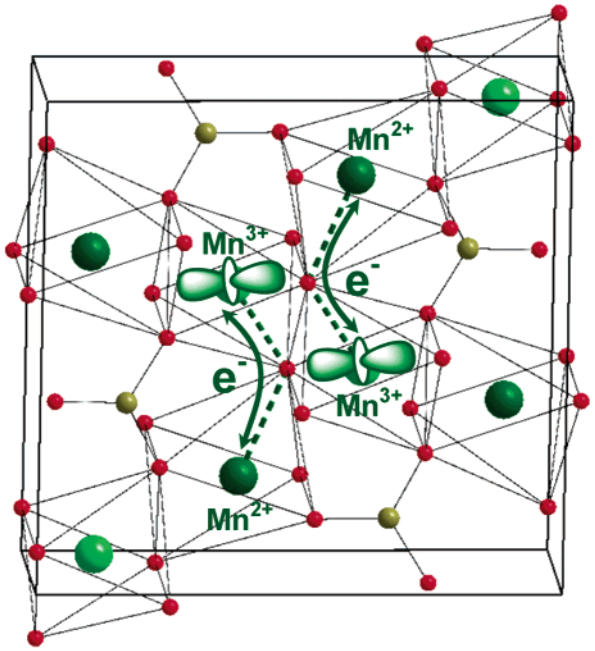

Figure 3. Schematic representation of the Mn^{3+}−O^{2-}−Mn^{2+} Zener Pairs in the Mn_2OBO_3. It is important to note that the two pairs are in different planes.

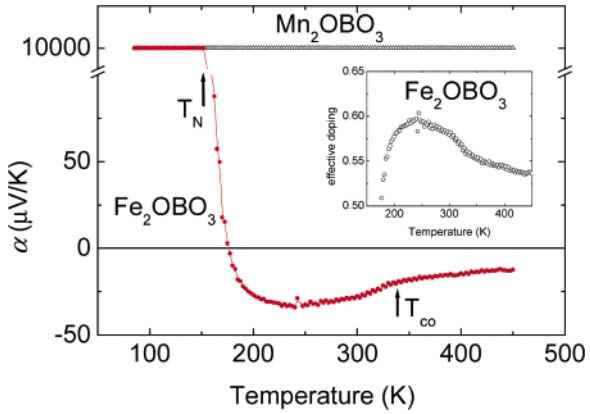

Figure 4. Thermoelectric power of Mn_2OBO_3 (open triangles) and Fe_2OBO_3 (closed circles). Inset: effective doping from thermopower in Fe_2OBO_3.

As a result of the crystallographic structure and the presence of the d_z^2 orbital ordering in the Mn^{3+} cation, the shared electron can only move inside the pair (see Figure 3), and as consequence, Mn_2OBO_3 is an insulator with an extremely large Seebeck coefficient (Figure 4).

Fe_2OBO_3. The thermal evolution of the ZFC−FC susceptibility for Fe_2OBO_3 is shown in Figure 5. The increase in the magnetization below $T_N = 155$ K marks the onset of

(14) Wertz, J. E.; Bolton, J. R. *Electron Spin Resonance: Elementary Theory and Practical Applications*; McGraw-Hill: New York, 1972.

(15) Causa, M. T.; Tovar, M.; Caneiro, A.; Prado, F.; Ibañez, G.; Ramos, C. A.; Butera, A.; Alascio, B.; Obradors, X.; Piñol, S.; Rivadulla, F.; Vázquez-Vázquez, C.; López-Quintela, M. A.; Rivas, J.; Tokura, Y.; Oseroff, S. B. *Phys. Rev. B* **1998**, *58*, 3233.

(16) Goodenough, J. B. *Prog. Solid State Chem.* **1971**, *5*, 145.

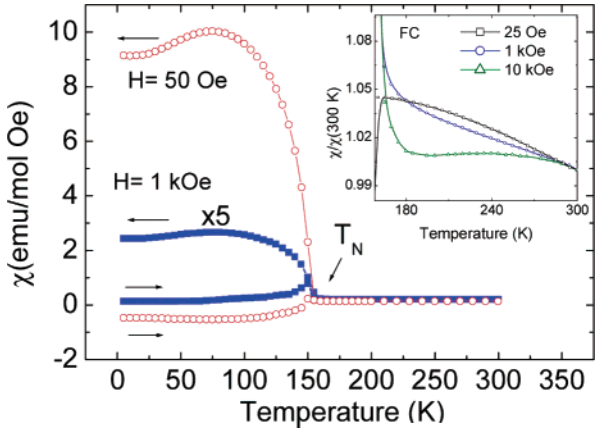

Figure 5. ZFC-FC susceptibility of Fe_2OBO_3 measured at two different fields, $H = 50$ Oe and $H = 1$ kOe, where the data corresponding to $H = 1$ kOe have been deliberately increased by a factor of 5 to facilitate their view. In the case of the ZFC−FC curves at $H = 50$ Oe, the sample was heated in a furnace at 373 K for 1 h followed by a cooling in a PPMS magnetometer with the ultralow field option. Inset: Detail of FC susceptibility measured at different fields in the high-temperature range.

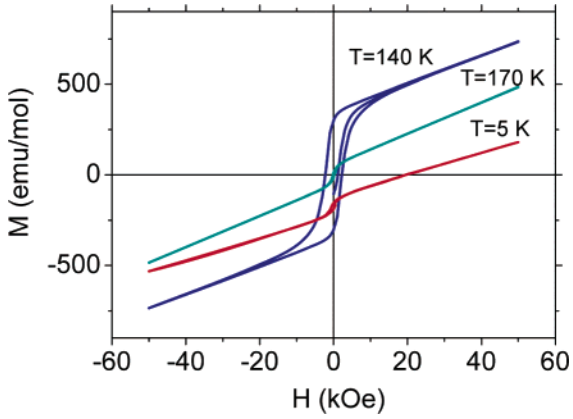

Figure 6. ZFC magnetization versus applied field H of Fe_2OBO_3 measured at three different temperatures, $T = 5$, 140, and 170 K.

long-range ferrimagnetic ordering, as previously reported.[6] Also the strong irreversibility between the ZFC−FC curves point to an inhomogeneous magnetic state (cluster-glass) below T_N.

The most unexpected result comes from the low field study of the magnetic susceptibility. After carefully measuring and removing the remnant field in the magnetometer, we have the ZFC Fe_2OBO_3 sample and measured the temperature dependence of its susceptibility under different fields from 9 to 100 Oe. The ZFC curve for $H = 50$ Oe is shown in Figure 5. The ZFC curve shows negative susceptibility below 155 K. Below this temperature and for fields smaller than 25 Oe, a remarkable magnetization reversal occurs, both in the ZFC and in the FC curves. For larger fields (up to 1−2 kOe) only the ZFC curve remains negative up to 155 K. We have verified this result by measuring again the magnetic properties of this sample after having first heated it in a furnace at 373 K (above the ordering temperature) for 1 h followed by a cooling in a PPMS magnetometer with the ultralow field option, which removes the residual field in the superconducting magnets and cools the sample in a field of less than 1 Oe.

We have to note that the results on the magnetic susceptibility of the Fe_2OBO_3 are in contradiction with those reported in ref 6. It could be due to two reasons: their sample could have been cooled in presence of remnant in the magnetometer, and/or another possible factor could be the presence of magnetite (around 5%); see experimental section of ref 6. This secondary phase is also contributing to the global magnetic signal, and this could hinder the observation of the true behavior of the oxyborate.

Three characteristic $M(H)$ cycles are shown in Figure 6. Saturation is never reached even under the highest magnetic field applied. On the other hand, the hysteresis loop at 5 K shows a large shift off the coordinates origin along the magnetization axis, crossing to positive values of M only for $H > 19\,300$ Oe.

Nevertheless, this effect is not observed in the curves obtained at $T = 170$ K (see Figure 6), that is, when the sample is not in the long-range magnetic ordering state.

This remarkable effect of magnetization reversal has been observed in different materials, in which two different spin-canting mechanisms tend to align the moments in an opposite direction.[17] For example, in YVO_3, the competition between single ion anisotropy and antisymmetric Dzyaloshinsky−Moriya interaction reverses the magnetization along different crystallographic directions.[18,19] Although this could be the source of magnetization reversal in Fe_2OBO_3, the competition between inter-ribbon versus intra-ribbon exchange interaction of different signs (and temperature dependences) cannot be discarded. In $Co^{2+}[Co^{2+}V^{4+}]O_4$, competition between $Co^{2+}-O-V^{4+}$ and direct $V^{4+}-V^{4+}$ cants the vanadium and cobalt spins in opposite directions, leading to a compensation point and magnetization reversal.[20] In any case, this point deserves further study before extracting any definitive conclusion.

On the other hand, between 155 and ≈300 K, we have observed a strong field dependence of the magnetic susceptibility (inset of Figure 5), which points to the presence of short-ranged magnetic interactions in this temperature interval. In fact, although a monoclinic distortion and an electrostatically driven charge ordering has been reported at $T_{CO} = 317$ K by Attfield et al.,[8] Mössbauer experiments[10] showed that charge ordering is not of long-range below T_{CO}.

In order to understand how the charge carriers localize across the structural transition at T_{CO}, we have performed thermoelectric power experiments across this temperature range (see Figure 4). At high temperature ($T > 320$ K), $\alpha(T)$ approaches asymptotically a temperature-independent value of ≈−12 μV/K, and it decreases only ≈ 2 μV/K in 100 K, so it can be considered practically temperature independent in this temperature interval. In this situation, thermoelectric power is reflecting the average entropy per carrier,[21] quantified by a statistical term of the form

$$\alpha = \pm \frac{k_B}{|e|} \ln\left[\beta \frac{1-c}{c}\right] \qquad (1)$$

where $c = x/N$ is the ratio of charge carriers (hole/electron)

(17) Kageyama, H.; Khomskii, D. I.; Levitin, R. Z.; Markina, M. M.; Okuyama, T.; Uchimoto, T.; Vasil'ev, A. N. *J. Magn. Magn. Mater.* **2003**, *262*, 445.
(18) Ren, Y.; Palstra, T. T. M.; Khomskii, D. I.; Pellegrin, E.; Nugroho, A. A.; Menovsky, A. A.; Sawatzky, G. A. *Nature* **1998**, *396*, 441.
(19) Yan, J.-Q.; Zhou, J.-S.; Goodenough, J. B. *Phys. Rev. B* **2005**, *72*, 94412.

to the number of sites available. Considering small polarons ($N = 1$) and $x = 0.5$, it will give $\alpha = 0$ μV/K. The value of $\alpha = -12$ μV/K observed experimentally could be due a small variation in the Fe^{3+}/Fe^{2+} ratio ($Fe^{3+}/Fe^{2+} = 1.13$). This off-stoichiometry could be related to the presence of defective intergrowths in the structure, as observed in high-resolution electron microscopy (HREM) images.[22] Below approximately 330 K, the thermoelectric power shows clear temperature dependence and increases its absolute value. Trapping out of mobile polarons by condensation into hole-poor bags which do not contribute to the conductivity renormalizes the statistics and introduces temperature dependence in eq 1. A simple condensation into localized two-site pairs (one electron for every pair of $Fe^{2+}-Fe^{3+}$) will not change the electron-to-site ratio in the small polaron matrix, and the thermopower will remain temperature independent. The hole-poor bags must represent short-range charge-ordered regions (probably AF ordered), and that is the most probable origin of the coexistence of delocalized and localized signals observed by Mössbauer in this intermediate temperature range. In previous reports the progressive increase in the resistivity below this temperature was interpreted as a CO transition into distinct Fe^{3+} and Fe^{2+} sites. However, in spite of the increase of the resistivity, the E_a does not change on crossing through T_{CO}.[9] That is because small polarons remain the charge carriers, although the number of available carriers is progressively reduced below what we signaled as T_{CO}.

Below 250 K there is a change in the curvature of the thermopower as the magnetic transition is approached. At $T_N = 155$ K the systems order magnetically; the divergence of $\alpha(T)$ below this temperature reflects a complete charge localization. The resistivity also increases abruptly below T_N. In view of this result, it seems that the Fe oxyborate has a real charge-ordering temperature at the Néel temperature $T_N = 155$ K, where AF order would prevent electron transfers through the t_{2g} orbitals. The electrostatic repulsion between electrons is not strong enough to drive a complete charge-localized state; spin ordering seems to be necessary for a complete charge ordering in this system.

As for the Mn_2OBO_3 compound, in the orthorhombic structure there are two different Fe−Fe distances inside the ribbons of Fe_2OBO_3 : a shorter $A^{2/3+}(1)-A^{2/3+}(1)$ distance (∼2.98 Å) and a longer $A^{2/3+}(1)-A^{2/3+}(2)$ distance (∼3.25 Å). At the structural transition at ∼317 K there is a decrease in the A(1)−A(1) distance and an increase in the A(1)−A(2) distance. Comparing these values with the critical distance for metal−metal bonding[16] (2.58 Å for $Fe^{3+}-Fe^{3+}$ and 2.95 Å for $Fe^{2+}-Fe^{2+}$), the A(1)−A(1) distance is close to the critical distances for the $Fe^{2+}-Fe^{2+}$ bonding so that in the Fe oxyborate metal−metal interactions are possible.

Therefore, for $T > 317$ K direct overlapping of $t_{2g}-t_{2g}$ orbitals would allow polaronic movement of the charge carriers. Around $T \approx 317$ K, the extra electron begins to condensate at the iron site and it drives to a crystallographic transition from orthorhombic (high temperature) to monoclinic (low temperature).

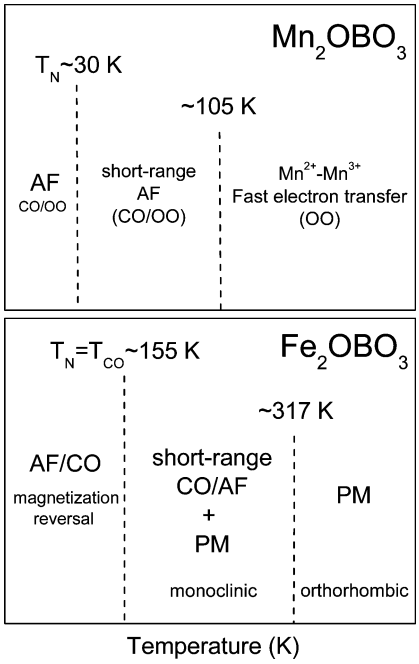

Figure 7. Schematic revised phase diagram proposed for Mn_2OBO_3 and Fe_2OBO_3.

Fe_2OBO_3 shows some similarities with magnetite Fe_3O_4, not only from the structural point of view. Fe_3O_4 shows a sharp decrease in conductivity[23] that is accompanied by a complex lattice distortion at 120 K. This is the so-called Verwey transition that has been interpreted as due to charge ordering of the Fe^{2+}/Fe^{3+} ions at the octahedral sites. Nevertheless, recent NMR[24] and X-ray resonant scattering results[25] proposed that the Verwey transition may not be a true charge ordering transition but a bond dimerization transition.

We think a similar process cannot be ruled out completely in Fe_2OBO_3 to explain the monoclinic−orthorhombic transition and the decrease in the conductivity at $T \approx 317$ K. In the magnetite the bond dimerization would take place directly through the t_{2g} orbitals, a situation that could be realizable in the case of the Fe oxyborate.

As a summary, in Figure 7, we show the revised phase diagrams we propose for Mn_2OBO_3 and Fe_2OBO_3 oxyborates.

Conclusions

From ESR, magnetization, and thermoelectric power on the isostructural Mn_2OBO_3 and Fe_2OBO_3, we have been able to establish important differences between the magnetic properties of these two compounds. In view of those results, we propose a revised phase diagram for both compounds.

We have rationalized the different behavior between Mn_2OBO_3 and Fe_2OBO_3 on the basis of their different

(20) Menyuk, N.; Dwight, K.; Wickham, D. G. *Phys. Rev. Lett.* **1960**, *4*, 119.
(21) Chaikin, P. M.; Beni, G. *Phys. Rev. B* **1976**, *13*, 647.
(22) Castro-Couceiro, A.; Sánchez-Andújar, M.; Señarís-Rodríguez, M. A. Unpublished results.
(23) Verwey, E. J. *Nature* **1939**, *144*, 327.
(24) Novak, P.; Stepankova, H.; Englich, J.; Kohout, J.; Braber, V. A. M. *Phys. Rev. B* **2000**, *61*, 1256.
(25) García, J.; Subías, G.; Proietti, M. G.; Blasco, J.; Renevier, H.; Hodeau, J. L.; Joly, Y. *Phys. Rev. B* **2000**, *63*, 54110.

electronic configurations. The physics of the Mn oxyborate is dominated by the strong tendency towards orbital ordering characteristic of a compound with a degenerate e_g electronic configuration.

On the other hand, the Fe oxyborate shows a very close relationship between CO/OO and magnetic ordering, typical of systems whose physics is dominated by interactions among t_{2g} orbitals.

Also, in the Fe sample the main interactions are though direct $t_{2g}-t_{2g}$ orbitals of neighbor cations. Meanwhile, in the case of the Mn sample, the Mn−Mn interactions are though e_g orbitals via sharing common O^{2-} anion. As the interactions in the Fe compound are stronger than in the Mn one, in the Fe sample the resistance is lower and the long-range magnetic ordering takes place at higher temperature than in the Mn compound.

In Mn_2OBO_3, we propose the possibility of a fast electron transfer between Mn^{2+} and Mn^{3+} cations. This situation is reminiscent of the formation of Zener polarons in the paramagnetic state of manganites, and it is certainly interesting to study this possibility in other materials in which $Mn^{(2+/3+)}$ pairs can exist.[26]

In the case of Fe_2OBO_3, we have observed the coexistence of short-range CO (probably AF ordered) with a paramagnetic state, below 317 K. Around $T = 155$ K the system becomes AF and the charge ordering becomes long-ranged.

Finally, the observation of low field magnetization reversal in Fe_2OBO_3 is an interesting phenomenon, observed in several metal oxides, which deserves further attention.

Acknowledgment. The authors are indebted to Prof. J.B. Goodenough for fruitful discussions. The authors wish to thank to M.J. Rosseinsky for his help in the synthesis of these compounds. The authors wish to thank the finantial support from DGICYT, Ministerio de Educación y Ciencia (Spain), and EU (FEDER) under Project No. MAT 2004-05130. F.R. acknowledges MEC of Spain for support under program Ramón y Cajal, M.S.-A. acknowledges Xunta de Galicia for support under program Parga Pondal, and B.R.-M. also wants to thank MEC of Spain for her FPI fellowship.

Supporting Information Available: Typical powder X-ray profile for the A_2OBO_3 samples (A = Fe, Mn), structural parameters for the A_2OBO_3 samples (A = Fe, Mn) and refined bond lengths according to Rietveld refinements of the XRPD data, additional ZFC and FC susceptibility curves corresponding to the Fe_2OBO_3 sample measured at low magnetic fields, and HREM image of a microcrystal Fe_2OBO_3 sample taken along the [100] zone axis (PDF). This material is available free of charge via the Internet at http://pubs.acs.org.

CM0609698

(26) Casey, P. S.; Barker, D.; Hayward, M. A. *J. Solid State Chem.* **2006**, *179*, 1375.